Pharm Res (2015) 32:482–491
DOI 10.1007/s11095-014-1476-2

RESEARCH PAPER

Preparation and Characterization of Cisplatin Magnetic Solid Lipid Nanoparticles (MSLNs): Effects of Loading Procedures of Fe_3O_4 Nanoparticles

Sha Zhao • Yongle Zhang • Yazhu Han • Jing Wang • Jie Yang

Received: 4 April 2014 / Accepted: 25 July 2014 / Published online: 30 August 2014

ABSTRACT

Purpose In order to improve formulation of targeting chemotherapy, cisplatin-loaded magnetic solid lipid nanoparticles (MSLNs) were prepared. In present study, the deliberate loading of Fe_3O_4 magnetic nanoparticles (MNs) into cisplatin SLNs was developed.

Methods SLNs were produced by film scattering ultrasonic technique. The effects of two different loading procedures of MNs on the microstructure and physicochemical properties of MSLNs were investigated by transmission electron microscopy (TEM), zetasizer, infrared spectroscopy (IR), and fluorescence spectroscopy. *In vitro* drug release and cytotoxicity against human cervical carcinoma SiHa cells, *in vivo* tumor cell uptake and target tissue distribution of MSLNs under external magnetic field were investigated.

Results The encapsulation efficiency of cisplatin and the content of MNs in procedure I SLNs were 69.20 ± 4.5% and 2.16 ± 0.53 mg/mL, respectively, which were higher than those of procedure II MSLNs. In procedure I, the MNs, which were combined with lipids during film formation, distributed in the middle of the lipid layer in SLNs. Differently, in procedure II, the MNs and cisplatin were contained in an interior compartment in SLNs, resulting from mixing with drugs during hydration of lipid film. The procedure I MSLNs had higher cytotoxicity than procedure II MSLNs or free cisplatin. With *in vivo* intratumoral administration, cisplatin concentration in the tumor tissue was maintained at higher level for MSLNs than that for free cisplatin, especially under external magnetic field.

Conclusions Procedure I, the developed deliberate MNs loading method, was superior over procedure II in cisplatin encapsulation efficiency, MNs content and cell cytotoxicity.

KEY WORDS cisplatin · cytotoxicity · encapsulation efficiency · MSLNs · targeting effect

ABBREVIATIONS

AAS	Graphite furnace atomic absorption spectrometer
DMSO	Dimethyl sulfoxide
EE	Encapsulation efficiency
F-68	Poloxamer 188
FBS	Fetal bovine serum
FT-IR	Fourier transform infrared spectroscopy
GMS	Glycerol monostearate
HSPC	Hydrogenated soybean lecithin
MNs	Magnetic nanoparticles
MSLNs	Magnetic solid lipid nanoparticles
MTT	3-[4,5-Dimethylthiazol-2-yl]-2,5-diphenyl-tetrazolium bromide
PBS	Phosphate-buffered saline
PDI	Polydispersity index
SLNs	Solid lipid nanoparticles
TEM	Transmission electron microscopy

INTRODUCTION

Cisplatin, a common clinical anticancer drug, is used as chemotherapy agent alone or in combination with other drug for the treatment of various solid tumors, for example, reproductive system tumors, head and neck tumors, as well as melanomas (1–3). Although many new cancer treatments chose

Electronic supplementary material The online version of this article (doi:10.1007/s11095-014-1476-2) contains supplementary material, which is available to authorized users.

S. Zhao • Y. Zhang • Y. Han • J. Wang (✉)
School of Pharmaceutical Sciences, Hebei Medical University, Shijiazhuang 050017, China
e-mail: jingwang@home.ipe.ac.cn

J. Yang (✉)
Preparation of the Third Hospital, Hebei Medical University, Shijiazhuang 050051, China
e-mail: qimiao88@126.com

cisplatin, it has serious side effects such as bone marrow suppression, nephrotoxicity, and neurotoxicity (4, 5). At present, the powder injection formulation of cisplatin is of therapeutic potential because of its easy oxidation and hydrolysis, light-unstable character, and short half-life of aqueous solution.

Solid lipid nanoparticles (SLNs), an alternative drug delivery system, is promising for improving cancer chemotherapy. The drawbacks frequently involved with anticancer drugs, such as above-mentioned normal tissue toxicity, poor stability, and a high incidence of drug-resistant tumor cells, can be relieved by SLNs delivering system. Compared with traditional carriers, SLNs have the advantages of both emulsions and polymeric nanoparticles for drug delivery, including good biocompatibility, low toxicity and targeting effect (6, 7). In addition, SLNs give more stable formulations and effectively prevent loaded unstable drug molecules decomposing and degrading. However, due to the polymorphic transformation of lipids, SLNs themselves possess some intrinsical deficiencies, for instance, gel formation, low drug loading and leaking, as well as low encapsulation efficiency. Accordingly, many efforts on modification of SLNs has been devoted to overcome these drawbacks for applications (8–10).

In recent years, as a new type of targeting drug delivery system, Magnetic SLNs (MSLNs) show effective application in cancer treatment. The loading of magnetic nanoparticles (MNs) permit the SLNs to get to the tumor target through blood circulation by magnetic field orientation (11, 12). Therefore, the toxicity as well as dosage decreased, reliability, validity and patient compliance is greatly improved.

In most cases, lipophilic drugs, showing good compatibility with the lipids matrix, were selected to load into the SLNs for high drug loading and high-level encapsulation (13–16). Instead, by virtue of their low encapsulation efficiency and drug loading, few investigations on SLNs focus on the hydrophilic drugs, typically, cisplatin, especially when MNs are loaded into the SLNs structure to occupy space. Hence, novel structural MSLNs for target delivery of cisplatin and high encapsulation efficiency are urgently needed.

The aim of present study was to evaluate the feasibility of preparing SLNs loaded with cisplatin and MNs by film scattering ultrasonic technique, and detect the drug encapsulation efficiency after deliberate loading of magnetic particles into cisplatin SLNs. The influence of different MNs loading procedures on the physicochemical properties of cisplatin loaded SLNs, such as particle size, zeta-potential, structure, drug entrapment efficiency were investigated in detail. Furthermore, *in vitro* drug release behavior and cell cytotoxicity, *in vivo* tumor cell uptake and target tissue distribution of MSLNs under external magnetic field were assessed.

MATERIAL AND METHODS

Materials

Cisplatin (purity >99%) was purchased from Kunming Guiyan, Pharmaceutical Co., Ltd., China. Glycerol monostearate (GMS) was supplied by Gracia Chemical Technology Co., Ltd. Chengdu, China. Hydrogenated soybean lecithin (HSPC; purity >98.0%) was purchased from Toshisum International Pty Ltd, Germany. F-68 was obtained from Jiqi pharmaceutical Co., LTD. Shenyang, China. SephadexG-50 was kindly donated by Pharmacia Fine Chemicals Co., Ltd., shanghai, China. Magnetic nanoparticles (Fe_3O_4) were prepared according to the Ref (17).

SiHa cell line (Human cervical carcinoma cell lines) was donated by Fourth Hospital, Hebei Medical University, Shijiazhuang, China. FBS (Fetal bovine serum), RPMI-1640 medium, phosphate-buffered saline (PBS, pH7.4), trypsin-EDTA solution were purchased from Gibco BRL, USA. Methylthiazolyldiphenyltetrazolium bromide (MTT, purity >99.0%) was obtained commercially from Tokyo chemical industrial co., Ltd., Japan. All other chemicals used were of analytical grade.

Methods

Optimization of Prescription with Orthogonal Experimental Design

According to the exploration of single factor experiment, four factors, which primarily effected the stability and drug entrapment efficiency, were identified as research objects, including the concentrations of GMS (A), HSPC (B), F-68 (C), and the ratio of lipid to magnetic nanoparticles (D, *w*/*w*). In order to obtain optimal formulations of prescription, each factor had three levels; nine pieces of prescription were applied based on $L_9(3^4)$ orthogonal experimental design. Used cisplatin encapsulation efficiency as screen index, the values of orthogonal array experiment was listed in Table 1.

Sample Preparation

Preparation of Cisplatin-Loaded SLNs. Cisplatin-loaded SLNs were prepared via the film scattering ultrasonic technique.

Table 1 Factors and levels of orthogonal experiment design

Levels	Factors			
	A	*B*	*C*	*D*
1	0.01	0.01	0.01	3:1
2	0.02	0.02	0.02	5:1
3	0.04	0.04	0.04	10:1

A: GMS (g/mL); B: HSPC (g/mL); C:F-68 (g/mL); D: (GMS + HSPC)/magnetic particle (g/g)

The specified amounts of GMS and HSPC were dissolved in chloroform. The mixture was evaporated using a rotary evaporator (60 r/min) at 42°C to form a homogeneous lipid film. Trace of solvent was removed by keeping the lipid film under a vacuum for 12 h. Then, the prepared lipid film was hydrated with 0.9% NaCl containing 2 mg/mL cisplatin for 2 h. The obtained solution was added to 0.9% NaCl solution containing desired amount of F-68. The suspension was sonicated at ambient temperature in a water bath for 2 h to produce the cisplatin-loaded SLNs.

Preparation of MNs-Loaded Cisplatin SLNs - Procedure I. Magnetic particles were dispersed in anhydrous alcohol under sonication for several minutes. Then, the suspension was mixed with chloroform solution containing lipids. The mixture was evaporated using a rotary evaporator (60 r/min) at 42°C to form homogeneous and magnetic lipid films, which were then processed as described above.

Preparation of MNs-Loaded Cisplatin SLNs - Procedure II. The specified amounts of GMS and HSPC were dissolved in chloroform. The mixture was evaporated using a rotary evaporator (60 r/min) at 42°C to form a homogeneous lipid film. The MNs and cisplatin were mixed in 0.9% NaCl solution to form MNs suspended cisplatin solution, which was used to hydrate lipid film.

Graphite Furnace Atomic Absorption Spectrometer (AAS)

The concentration of cisplatin were measured by Hitachi Z-2000 (Tokyo, Japan) graphite furnace atomic absorption spectrometer (AAS). The instrumental operating conditions were as follows: Argon was used as protect gas at the rate of 200 mL/min; lamp current was 6 mA; the wavelength of the light was 265.9 nm; slit width was 0.4 nm; injection volume was 10 μL.

Transmission Electron Microscopy (TEM)

The morphology of the cisplatin-loaded MSLNs were assessed by a TEM system (HITACHI H-7650). The MSLNs suspension was deposited drop wise on a copper grid coated with carbon film, and then dried and stained with 2% phosphotungstic acid

Particle Size and Zeta Potential Measurements

The measure of mean particle size and polydispersity index (PDI) of MSLNs suspension were performed by dynamic light scattering technique using a Zetasizer (Nano-ZS90, Malvern Instruments, UK). The MSLNs suspension was diluted with distiller water (1:100) and stirred in order to minimize light scattering (18). The zeta potential was measured by the nanoparticles electrophoresis mobility using a U-type tube at 20°C. All samples were in triplicate to obtain the mean value.

Fourier Transform Infrared Spectroscopy (FT-IR)

All experiments were carried out on a FT-IR spectrometer (Shimadzu, FT-IR-8400S). MSLNs suspension was dried under a vacuum condition at room temperature to form powder. Each IR spectrum was recorded from wave number 4,000 to 400 cm^{-1} under the average of 30 scans with a spectral resolution of 4 cm^{-1}; the spectral peak accuracy was of 0.01 cm^{-1}. The IR spectra were recorded and stored via spectroscopic software (OPUS, Version2.0). The FT-IR spectra of the pure substances were obtained by mixing 4 mg of the dried solid substance in an agate mortar with 160 mg of desiccated IR grade KBr (Merck) in a dry box.

Fluorescence Measurements

The fluorescence measurements were accomplished by a spectrofluorometer (FS-380,Tianjin, China). Pyre, as lipophilic photo physical probe, was blended with lipids in chloroform to form a lipid film during the preparation of MSLNs. The pyre-labeled MSLNs suspension was injected into the stopped flow chamber to measure the fluorescence intensity at room temperature. The determination conditions were as follows: the excitation wavelength was set to 337 nm; the emission wavelength was recorded in the range of 350–450 nm; the slits of the emission and excitation were both 5 nm. Each measurement was performed at least thrice to ensure the reproducibility of the experimental kinetic traces.

The Encapsulation Efficiency of Cisplatin and MNs

Un-entrapped drug was separated by size exclusion chromatography on a Sephadex G-50 column using double distilled water as the eluent. Each fraction was collected and measured by AAS system (Hitachi, Z-2000). The encapsulation efficiency (EE) of drug was calculated as below:

$$EE(\%) = (1 - W_f/W_t) \times 100\%$$

Where W_f represented the amount of un-entrapped drug and W_t is the total amount of cisplatin before treatment.

The amount of MNs loaded into the MSLNs was determined by the 1,10-phenanthroline monohydrate dyeing method, based on the Fe (II) and 1,10-phenanthroline monohydrate forming an orange complex under a pH value of 4–5 using a UV–vis spectrophotometer (TU-1901) (19).

In Vitro Drug Release

Drug release from SLNs study was carried out in a Franz diffusion cell. A regenerated cellulose membrane with a molecular weight cut off 8,000–12,000 Da (MD 25, USA) was used. 1 mL of SLNs suspension was contained in the donor

compartment of the cellulose membrane. The receptor compartment was filled with 0.9% NaCl solution. The cellulose membrane and 50 mL of 0.9% NaCl solution were set into Erlenmeyer flask, which was placed in an incubator shaker (THZ-8A, Jiangsu, China) at 37°C and horizontally shaken at 75 rpm. At definite time intervals, 2 mL aliquots of the receptor medium were withdrawn and immediately replaced with fresh equal volume of the release medium. The drug concentration was determined by AAS in the same way of encapsulation efficiency. All drug release tests were performed thrice.

To determine the drug release mechanism from SLNs, drug release kinetics were investigated by applying kinetics models on drug release data to find the best fitting equations (20).

Statistical Analysis

In vitro drug release from SLNs was analyzed by nonparametric Mann–Whitney test. 0.05 level of probability was taken as the minimal level of significance.

In Vitro Cytotoxicity Tests

The *in vitro* cytotoxic activity of cisplitin solution, cisplitin loaded SLNs and MSLNs against human cervical carcinoma SiHa cells was assessed by MTT method. SiHa cells was incubated in RPMI 1640 medium containing 10% FBS and 1% pencillin-streptomycin in a humidified atmosphere of 5% CO_2 in air at 37°C. Cells was subcultured regularly with trypsin/EDTA. Briefly, 5×10^3 cells/well in growth medium were plated in 96 well plate (Jet Bio-chemical Int'l., Inc, Canada) and grown for 24 h. Then the cells was exposed to 20 μL different concentrations of cisplitin solution, MNs- free SLNS and cisplitin loaded MSLNs, respectively, for another 24 h and 48 h. At the end of incubation time, the cells was washed with PBS, then 20 μL 5 mg/mL 3-[4,5-dimethylthiazol-2-yl]-2,5-diphenyl-tetrazoliu bromide (MTT) was added, and incubated for further 4 h. Then, 150 μL DMSO was added to dissolve formazan crystals resulting from MTT reduction. Finally, the plates were gently shaken for 10 min, and the absorbance of formazan product was measured spectrophotometrically in an ELISA reader (Tecan, Sunrise Romote) at 490 nm. All the experiments were performed instantly. Cytotoxicity was evaluated by cell inhibition.

In Vivo Intratumoral Administration Under External Magnetic Field

The solid tumors were obtained by a subcutaneous injection of 4×10^6 human cervical carcinoma SiHa cells into the armpit of female nude mice (B AIB/C, 6 weeks old, Certificate No.0043433). The nude mice were purchased from the Laboratory Animal Center, Academy of Military Medical Sciences, Beijing, China and were housed under pathogen-free conditions according to Fourth Hospital of Hebei Medical University animal care guidelines. All animal experiments were reviewed and approved by the Animal Care Committee at Hebei Medical University. After 2 weeks, the size of the tumors had grown to approximately 7 mm diameter. 12 tumor-bearing model mice were randomly divided into three groups (group A, B, and C) with each group consisting of 4 animals. The animals of the group A were intratumorally injected free 0.1 mL cisplitin aqueous solution (with about 50 mg cisplatin). For the animals of the group B (with external magnetic field group), the tumor parts were fixed by cylindrical rubidium iron boron rare earth magnet (diameter 10 mm×10 mm, surface field strength of 4500 gauss) before injection. Both the groups B (with external magnetic field group) and C (without external magnetic field group) were intratumorally injected 0.1 mL MSLNs (with 50 mg cisplatin). After 12 h, the tumor sites of all the mice were cut away and weighed for determination accumulation amount of cisplatin within tumors.

Each tumor tissue was homogenized in two folds amount of 0.9% NaCl solution. Enough methanol was added to the serum and homogenate to precipitate the proteins respectively. Subsequently, the contents were vortexed for 3 min and then centrifuged at 14,000 rpm for 15 min. The supernatants were evaporated under nitrogen at room temperature. The leftover residue was dissolved in 500 μL 0.9% NaCl solution. Concentration of cisplatin was determined using AAS according to the previously reported method.

In Vivo Target Tissue Distribution of MSLNs Under External Magnetic Field

Kunming mice (male), weighting 18–22 g, with no prior drug treatment, were obtained from Hebei Experimental Animals Centre of Hebei Province, China. All mice were kept in fasted overnight before the experiments but had free access to water. Ten mice were randomly divided into two groups (group A and group B) with each group consists of five animals. The animals of group B were shaved the hair in the upper left abdomen and the left kidney parts were fixed cylindrical rubidium iron boron rare earth magnet (diameter 10 mm× 10 mm, surface field strength of 4,500 gauss). The MSLNs suspension was injected intravenously into the tail vein of the mice in a dose equivalent to 0.6 mg/kg bodyweight for both group A and group B animals. After half an hour, the magnets were removed from the group B animals. Blood was sampled from mice eyes, then the mice were sacrificed by cervical dislocation and organs of interests such as liver, heart, kidneys, brain were quickly removed, washed with 0.9% NaCl, snap-frozen and stored at −20°C until later analysis.

The blood samples were centrifuged at 4,000 rpm (LG16-B,Beijing,China) for 10 min and the serum was separated spare.

Each tissue organ was treated in the same way as for tumor tissue that was reported previously. Concentration of cisplatin in serum and various tissues was determined using AAS.

RESULTS AND DISCUSSION

Results of Orthogonal Experimental Design and Drug Encapsulation Efficiency

The physicochemical properties of the cisplatin loaded SLNs prepared via different procedures were measured by assessing drug encapsulation efficiency, mean diameter, and profiles. The results of orthogonal experimental design were listed in Table 2. As the results suggested, the range that reflected the extent of each factor affecting on encapsulation efficiency was bigger; the affected extent was greater. By range analysis, four factors in the present study were arranged as D>A>C>B. The bigger comprehensive mean value was, the higher rank it referred to. Based on comprehensive mean value, the optimized level combination of every factors was selected. Analytic results of four factors were, A:1>2>3; B:3>2>1; C:2>3>1; D:1>2>3. According to the factors and levels of orthogonal experiment design in Table 1, the best experimental combination was made for the optimal level of every factor combined, that was $A_1B_3C_2D_1$, i.e., GMS=0.01 g/mL, HSPC=0.04 g/mL, F-68=0.02 g/mL, (GMS + HSPC)/magnetic particles=3:1 (g/g). Preparation artwork: temperature of the lipid film formation by rotary evaporator (42°C), hydration time (2 h), ultrasonic emulsification time (2 h) under ambient temperature.

Table 2 Results of orthogonal experiment and direct-viewing analyses

No.	Factors				EE (%)
	A	B	C	D	
1	1	1	1	1	55.45
2	1	2	2	2	59.80
3	1	3	3	3	47.05
4	2	1	2	3	44.43
5	2	2	3	1	51.82
6	2	3	1	2	53.70
7	3	1	3	2	47.87
8	3	2	1	3	39.00
9	3	3	2	1	57.61
K1	54.100	49.250	49.383	54.960	
K2	49.983	50.207	53.947	53.790	
K3	48.160	52.787	48.913	43.493	
R	5.940	3.537	5.034	11.467	

A: GMS (g/mL); *B*: HSPC (g/mL); *C*:F-68 (g/mL); *D*: (GMS + HSPC)/magnetic particle (g/g)

Based on the results of orthogonal experimental design, the optimal experimental combination was adopted to synthesize the SLNs for evaluation of the drug encapsulation efficiency. The average encapsulation efficiency of the procedure I MSLNs was 69.20±4.5%, while the procedure II MSLNs and the MNs-free SLNs entrap the cisplatin of 57.65±3.2% and 46.16±3.7%, respectively. The content of Fe_3O_4 MNs in procedures I and II MSLNs are 2.16±0.53 and 2.00±0.91 mg/mL respectively. Indubitably, the procedure I is superior over procedure II in both cisplatin encapsulation efficiency and MNs content. Furthermore, it was shown that loading of magnetic Fe_3O_4 MNs into the SLNs was beneficial to the encapsulation of cisplatin. For procedure I MSLNs, the higher encapsulation efficiency of cisplatin may result from the increased disorder of lipid layer in MSLNs. As it's well known, for SLNs, the crystallization degree, order of lipid and stabilizer are the main factors that can affect the encapsulation efficiency of drugs, that is, the higher the crystallization degree is, the higher is the order of the lipid structure, and the lower is the encapsulation efficiency for drugs (21). When Fe_3O_4 nanoparticles, which are doped with organic groups (17), are loaded in the lipid layer, the order of the lipid layer (including lipid and emulsifier) decreases and the disorder increases, leading to the higher encapsulation efficiency of drugs. It was verified by fluorescence spectra (*vide infra*) that the microenvironment of the lipid layer changed when Fe_3O_4 nanoparticles were introduced. In our research team, a novel DPPC: M^{2+} delivery system for cisplatin thermosensitivity liposome with improving loading efficiency was developed (*unpublished manuscript*). In this novel delivery system, metal ions were introduced into the bilayer of liposome to affect the microstructure of bilayer for the aim of decreasing its order, as a result, the loading efficiency for cisplatin was successfully improved by the DPPC: M^{2+} novel delivery system. These findings indicate that doping can increase the disorder of the lipid layer, as a result, improve loading efficiency of drugs. For procedure II MSLNs, in which Fe_3O_4 nanoparticles were contained in an interior compartment in SLNs, the higher encapsulation efficiency of cisplatin may attribute to the adsorption of cisplatin onto the surface of Fe_3O_4 nanoparticles, which have larger surface area (about 10 nm diameter) and great adsorption ability. When Fe_3O_4 nanoparticles were mixed with cisplatin solution in procedure II, with the introduction of Fe_3O_4 nanoparticles into the SLNs, the loading concentration of cisplatin into the SLNs increases by adsorbing onto the surface of Fe_3O_4 nanoparticles.

TEM and Particle Size of SLNs

A visual inspection of SLNs prepared by different procedures from TEM micrograph reveals that the products are homogeneous, regular and spherical morphology, as shown in Fig. 1. The mean particle size, PDI and zeta potential of

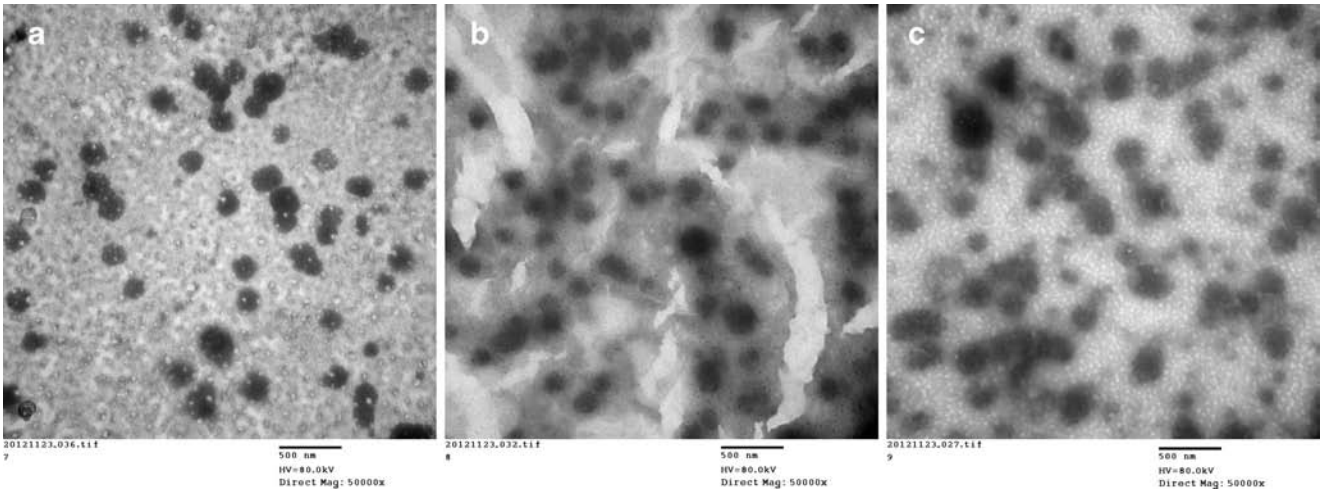

Fig. 1 TEM micro-photo of cisplatin-loaded SLNs. (**a**): MNs-free SLNs; (**b**): Procedure I MSLNs; C: procedure II MSLNs.

MNs-free SLNs, procedure I and II cisplitin-loaded MSLNs are listed in Table 3.

The mean diameter of procedure I MSLNs is smaller than those of MNs-free SLNs and procedure II MSLNs, which is consistent with the observation by TEM (Fig. 1). The high PDI reflecting wide size distribution maybe related to the formation of other structures such as liposomes, micelles, nanosuspensions or polycystic phospholipid layers (22, 23). Zeta potential is a key factor to estimate the stability of colloidal dispersion. It was currently admitted that zeta potentials ≥30 mV or ≤−30 mV were required for electrostatic stabilization due to the electric repulsion between particles. It was also reported that the zeta potential between 5 mV and 15 mV led to limited flocculation, oppositely, the value between −5 mV and 3 mV resulted in maximum flocculation (24). The negative zeta potential reveals that surface-active agent with negatively charged head groups stabilizes the lipid through absorbing on the surface, which provides electrostatic force. As shown in Table 3, the zeta potential of as-prepared SLNs was well within the range of electrostatic stabilization. It verified by stability experiment that the as-prepared SLNs remain stable against aggregation at 4°C for 30 days (data not shown). The zeta potential less than −30 mV maintain SLNs dispersing uniformly in the system. Furthermore, the zeta potential of MNs-free SLNs and procedure II MSLNs are nearly equal, but different from that of procedure I MSLNs, indicating that microstructure of procedure I MSLNs differs from that of the other two.

Table 3 The diameter and zeta potential of cisplatin loaded SLNs

	Diameter (nm)	Zeta potential (mV)	PDI
MNs-free SLNs	256.5 ± 2.01	−33.34 ± 0.45	0.39 ± 0.03
Procedure I MSLNs	224.0 ± 1.42	−35.18 ± 0.42	0.37 ± 0.02
Procedure II MSLNs	253.4 ± 1.22	−33.64 ± 0.95	0.52 ± 0.01

FT-IR Spectra

The FT-IR spectra of the SLNs were recorded between 4,000 and 400 cm^{-1} (Fig. 2) to investigate the interaction of MNs and lipid matrix. One strong (3400 cm^{-1}) absorption band is observed for hydroxyl (O-H) stretching vibration of GMS. The bands at 2,920 and 2,850 cm^{-1} are attributed to the symmetric and asymmetric vibrations of methylene ($-CH_2$) as well as methyl ($-CH_3$) (25). Phosphatide acyl of the HSPC is electrically charged, so the interaction between lipid matrix and MNs could be evaluated by researching the characteristic peaks of polar groups in 1800 ~ 400 cm^{-1} (26).

The bands at 1,242 and 1,112 cm^{-1} are attributed to symmetric and asymmetric phosphorus (PO_2^-) in HSPC; the bands at 840 and 764 cm^{-1} may assign to the antisymmetric and symmetric stretching vibration band of the P-O-C groups; the bands around 600-500 cm^{-1} are due to the in-plane flexural vibration of PO_2^- groups. It can be seen from Fig. 2, the intensity of bands associated with the vibration of phosphatide acyl decreased with the introduction of MNs into the SLNs, especially in procedure I MSLNs. It indicates that

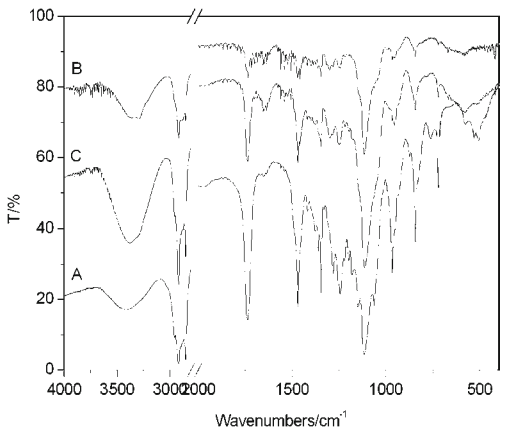

Fig. 2 FT-IR spectra of SLNs. (**a**): MNs-free SLNs; (**b**): Procedure I MSLNs; (**c**): Procedure II MSLNs.

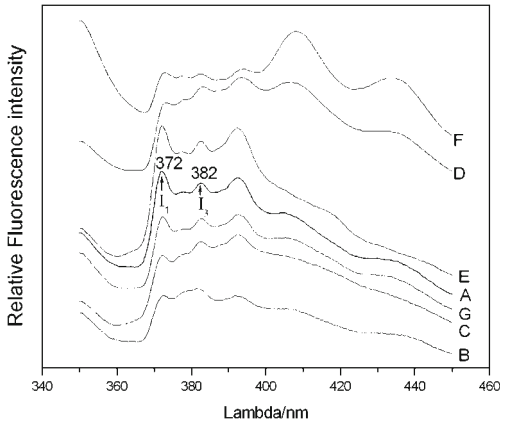

Fig. 3 Fluorescence spectra of pyrene-labelled SLNs and MSLNs MNs-free SLN for (**a**); Procedure I MSLNs with the ratio of (GMS + HSPC)/MNs 3:1 for (**b**), 5:1 for (**c**), and 10:1 for (**d**); Procedure II MSLNs with the ratio of (GMS + HSPC)/MNs 3:1 for E, 5: 1 for F, and 10:1 for G.

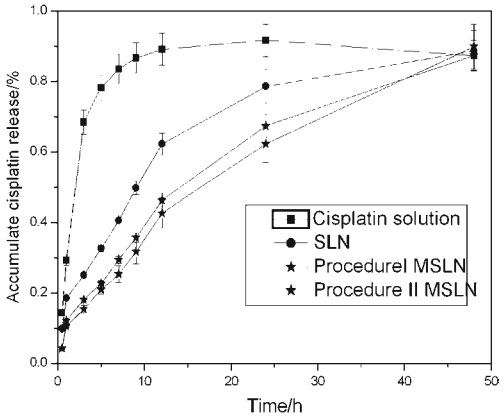

Fig. 4 The release profile of cisplatin from the MSLNs and cisplatin solution *in vitro* ($n = 3, \bar{x} \pm s$).

weak interactions between lipid polar groups and MNs charged with surface charge occurs in MSLNs, which is not enough to change the vibration frequency in IR, but decreases the intensity of vibration of phosphatide acyl polar groups. More decreasing intensity vibration of polar groups suggests stronger interaction between lipid polar groups and MNs in procedure I MSLNs.

Fluorescence Spectra

The different structures of SLNs, procedure I and II MSLNs were explored by fluorescence spectra. Pyrene, serverd as probe, has the key feature of the solvent dependent variation in the ratio of its fine structure emission band intensities, which are associated with the polarity of the immediate environment of the probe. The characteristic excimer emission of the pyrene is used to assess its concentration in the environment of emitting probe placed (27). The fluorescence spectra of pyrene-labelled SLNs and procedure I and II MSLNs with different concentration of MNs are shown in Fig. 3. The fluorescence intensities of pyrene-labelled MSLNs significantly decrease due to the fluorescence quenching caused by super-paramagnetic Fe_3O_4, especially in procedure I MSLNs, in which more MNs are loaded. Pyrene, a lipophilic compound, is embedded in the hydrophobic lipid matrix in MSLNs, the variability of the ratio of the first (372 nm) and third (382 nm) vibration absorption band fluorescence intensities (I_1/I_3) of the pyrene-labelled SLNs indicates the difference in the hydrophobic microenvironment of the lipid matrix. When the MNs are loaded into the SLNs by a model of embedding in lipid matrix, they could change the hydrophobic environment of the lipid matrix due to the effects of steric hindrance and static electricity. While, the hydrophobic environment of pyrene in the lipid matrix has no obvious change if the MNs are trapped in an interior compartment in SLNs. The values of I_1/I_3 of pyrene-labelled of SLNs, procedure I and procedure II MSLNs are listed in Table 4. The change of the values of I_1/I_3 of pyrene-labelled MSLNs proves that the MNs are embedded into the lipid matrix in procedure I, and trapped in an interior compartment in procedure II MSLNs. The surface adsorption character is affected by entrapping the MNs into the lipid matrix of procedure I MSLNs, and has no obvious change in procedure II MSLNs. This conclusion is consistent with the result of the zeta potential.

Table 4 Peak intensity ratios (I_{372}/I_{382}) of fluorescence of pyrene-labelled SLNs and MSLNs

(GMS + HSPC)/MNs (g/g)	Procedure I MSLN	Procedure II MSLN	MNs-free SLN
3:1	0.93	1.07	1.06
5:1	0.92	1.04	
10:1	0.94	1.03	

In Vitro Drug Release Characters of SLNs

To study the drug release characteristics from the SLNs, the amount of cisplatin released from each SLNs system is plotted as a function of time (Fig. 4). To provide sink conditions, the aqueous solution of 0.9% NaCl is chosen as a receptor medium. The cisplatin solution releases approximately 50% in 2.4 h, while the MNs-free SLNs, procedure I and II release cisplatin approximately 50% in 8.7, 14 and 12.5 h, respectively. The release of cisplatin from the three kinds of SLNs all display an initial burst, indicating that some drug molecules

Table 5 Regression equation of SLNs release *in vitro*

Sample	Regression equation	R^2
MNs-free SLNs	$\ln\ln [1/(1-M_t/M_\infty)] = 0.6642 \ln t - 1.8068$	0.9779
Procedure I MSLNs	$M_t/M_\infty = 6.8455\ t^{1/2} + 0.5735$	0.9801
Procedure II MSLNs	$\ln\ln [1/(1-M_t/M_\infty)] = 0.8199 \ln t - 2.4408$	0.9680

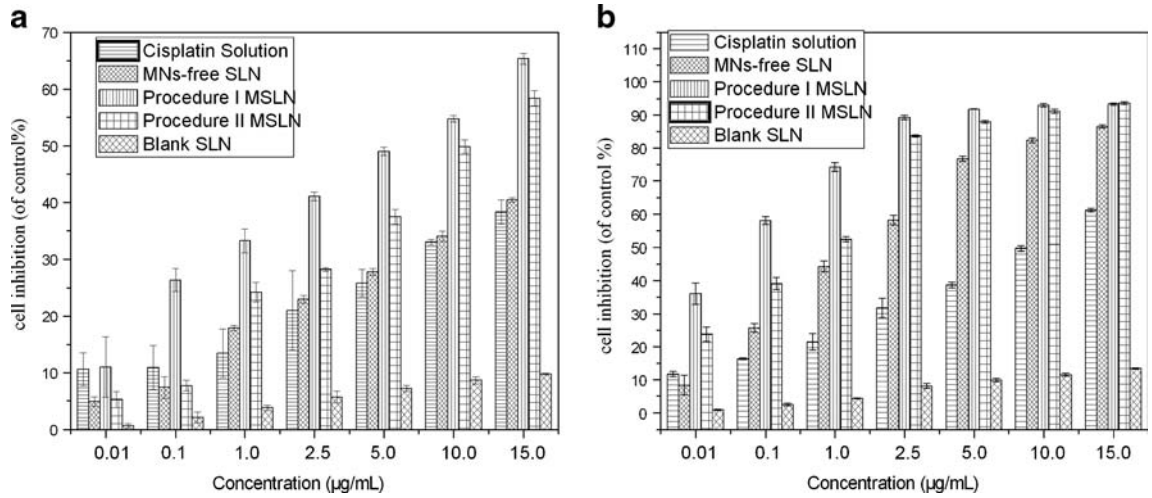

Fig. 5 Cell inhibition rate following treatment with cisplatin in 0.9% NaCl solution, MNs-free SLNs, MSLNs, and blank SLN after incubation for 24 h (**a**) and 48 h (**b**) Each value represents the mean and S.D. ($n = 3$).

are adsorbed or deposited on the surface of SLNs with large surface area in the process of formation. After initial burst release, the drug entrapped in interior compartment of SLNs shows sustained releasing from the skeleton of SLNs. Both MSLNs prepared by procedures I and II show slower release characters than the MNs-free SLNs ($P < 0.05$). When MNs are introduced into the structure of SLNs, the magnetic attraction between the adjacent SLNs slows the drug release *in vitro* (20).

The regression kinetic equations of drug release were fitted according to different models, including zero-order, first-order, Higuchi and Weibull models (28). The equations and correlation coefficients (R^2) are listed in Table 5. Depending on the goodness-of-fit test, the data of cisplatin release from the MNs-free SLNs and procedure II MSLNs best fit the ideal Weibull model. However, release data from the procedure I MSLNs fits Higuchi model, indicating that diffusion seems to be the main factor for controlling the release of the encapsulated cisplatin from procedure I MSLNs (20). The difference of regression kinetic equations of drug release from procedures I and II MSLNs also indicates the difference in microstructure of the two MSLNs.

In Vitro Cytotoxicity Assayt

The 24 and 48 h-cytotoxic effects of cisplatin solution, MNs-free SLNs, and MSLNs against SiHa (human cervical carcinoma cell line) cells were experimented by MTT method. The cytotoxic effects of cisplatin-loaded SLNs and cisplatin solution on the inhibition of SiHa cells are presented in Fig. 5 and the corresponding IC_{50} of cisplatin are listed in Table 6. The SiHa cell inhibition rates increase with the concentration of cisplatin, indicating that the cytotoxicity showed an obvious dose-dependent effect. Importantly, cisplatin-loaded MNs-free SLNs as well as two cisplatin-loaded MSLNs showed higher antitumor activity than free cisplatin solution. The ultimate goal of effective delivery of cisplatin can be fulfilled only if it is able to localize and integrate with DNA in tumor cell. Owing to the poorly lipophilic character, the cisplatin aqueous solution is poorly permeable through cell membranes (29). Cellular uptake of cisplatin can possibly occur by an endocytotic pathway of lipophilic SLNs vesicles or by fusion of SLNs surfaces with the tumor cell membrane. Although there seem to be several mechanisms responsible for

Table 6 The IC_{50} of cisplatin from the SLNs and 0.9% NaCl aqueous solution at 24 h and 48 h against SiHa Cells

IC_{50} (μg/mL)	Cisplatin solution	MNs-free SLNs	Procedure I MSLNs	Procedure II MSLNs
24 h	19.88 ± 2.43	17.92 ± 0.72	8.25 ± 0.97	10.84 ± 1.41
48 h	10.35 ± 0.87	0.72 ± 0.03	0.04 ± 0.003	0.20 ± 0.05

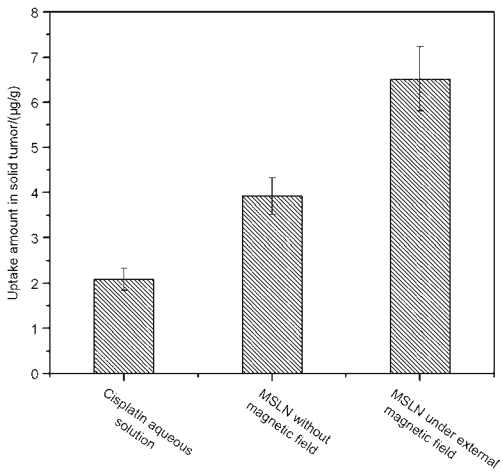

Fig. 6 *In vivo* cumulative uptake of cisplatin in solid tumor at 12 h from an cisplatin aqueous solution and MSLN (without or with external magnetic field: diameter 10 mm × 10 mm, surface field strength of 4,500 gauss) after an intratumor injection into tumors on the armpits of nude mice. Each value represents the mean and S.D. ($n = 4$).

Table 7 The concentration of cisplatin in brain, heart, liver and kidney (μg/mL or μg/g, $\bar{x} \pm s$, $n = 5$)

Group	Plasma	brain	Heart	Liver	Left kidney	Right kidney
A	22.69 ± 1.12	25.20 ± 1.25	55.35 ± 1.54	47.37 ± 0.84	24.15 ± 1.31	21.54 ± 1.72
B	24.04 ± 1.39	7.74 ± 1.36	33.54 ± 2.39	76.05 ± 3.06	67.23 ± 1.97	15.24 ± 0.87

internalization of lipophilic SLNs vesicles, it was suggested that endocytosis is the major way (30, 31). So, the higher the encapsulation efficiency of SLNs is, the easier uptake of cisplatin into tumor cell can be achieved.. This conclusion is supported by the fact that the procedure I MSLNs show higher cell inhibition rate than that of other SLNs, attributing to their relative higher cisplatin encapsulation efficiency. Correspondingly, the IC_{50} value of procedure I MSLNs is the lowest one in all samples after 24, 48 h administration (Table 6). Furthermore, the cytotoxicity of SLNs shows a period-dependent effect. 24 h administration with 0.01 μg/mL cisplatin concentration for SLNs or MSLNs was not sufficient compared with free cisplatin to induce apoptosis in SiHa cells, while, all MSLNs showed higher cytotoxic activity than free cisplatin after 48 h administration, even at low drug concentration. It indicated that the release of drug from SLNs spent more time than free drug.

In Vivo Tumor Cell Uptake Under External Magnetic Field

In order to examine *in vivo* tumor uptake of cisplatin aqueous solution and MSLNs (with or without external magnetic field), free cisplatin aqueous solution or incorporated within MSLNs was intratumorally injected into tumor on the armpits of nude mice. Fig. 6 shows the cumulative uptake of cisplatin in solid tumor at 12 h after the injection. Cisplatin accumulation within the solid tumors was low in the group of free cisplatin aqueous solution. The same as findings *in vitro* cytotoxicity assay, the uptake amount of cisplatin into the tumor tissue cell increased when cisplatin was incorporated within MSLNs. Furthermore, owing to the prolonging the retention time at tumor location by the external magnetic field, MSLNs showed the most superior effect on the increase in cisplatin accumulation within tumor cell under magnetic field.

In vivo Target Tissue Distribution of MSLNs

The tissue distributions of the MSLNs after intravenous administration at 30 min are shown in Table 7. For group B, which were fixed external magnetic field to t;he left kidney, the content of cisplatin are significantly higher than that in the right kidney ($P = 0.09 > 0.05$) after 30 min tail vein injection of MLSNs, indicating obvious magnetic targeting effect of MSLNs *in vivo*. On the contrary, the drug content in the two kidneys is not significantly different ($P = 0.056 > 0.05$) for the group A (without external magnetic field). Furthermore, owing to affecting by adjacent magnetic field, the concentration of cisplatin in liver of group B is higher than that of group A. Moreover, just because of higher concentration of drug in the tissues locating adjacent magnetic field, the concentration of drug in tissues that are far from the magnetic field, such as brain and heart, is reduced for group B. The results demonstrate that MSLNs, as the cisplatin carrier, can carry the cisplatin to target area under external magnetic field.

CONCLUSION

The purpose of this study is to explore the deliberate loading of magnetic particles in cisplatin-loaded SLNs to overcome the drawback of low encapsulation efficiency and achieve targeting delivery of the drug. A comparation was made between two different loading procedures of magnetic particles on the physicochemical properties and structure of cisplatin loaded MSLNs. The loading of magnetic particles into the lipid layer of SLNs was actualized using procedure I, in which lipids combined with magnetic particles before the formation of the lipid film. The resulting magnetic SLNs significantly increased the entrapping efficiencies of cisplatin and magnetic particles, maintained the sustained release of cisplatin from MSLNs, meanwhile, showed a high cytotoxicity *in vitro* and obvious magnetic targeting effect *in vivo*.

ACKNOWLEDGMENTS AND DISCLOSURES

The financial support for this work by the Hebei Provincial Natural Science Fund of China (H2013206040, 2008001072) is greatly acknowledged.

REFERENCES

1. Ali BH, Al-Moundhri MS. Agents ameliorating or augmenting the nephro-toxicity of cisplatin and other platinum compounds: a review of somerecent research. Food Chem Toxicol. 2006;44(8):1173–83.
2. Marchion DC, Xiong Y, Chen N, Bicaku E, Stickles XB, *et al.* The BCL2 antagonist of cell death pathway influences endometrial cancer cell sensitivity to cisplatin. Gynecol Oncol. 2012;124(1):119–24.
3. Mitsudomi T, Morita S, Yatabe Y, Negoro S, Okamoto I, Tsurutani J, *et al.* Gefitinib *versus* cisplatin plus docetaxel in patients with non-small-cell lung cancer harbouring muta-tions of the epidermal growth factor receptor (WJTOG3405): an open label, randomised phase 3 trial. Lancet Oncol. 2010;11:121–8.

4. Kuang Y, Liu J, Liu ZL, Zhuo RX. Cholesterol based anionic long-circulating cisplatin liposomes with reduced renal toxicity. Biomaterials. 2012;33(5):1596–56.
5. Qu J, Li X, Wang J, Mi WJ, Xie KL, Qiu JH. Inhalation of hydrogen gas attenuates cisplatin-induced ototoxicity via reducing oxidative stress. Int J Pediatr Otorhinolaryngol. 2012;76(1):111–5.
6. Li H, Zhao X, Ma Y, Zhai G, Li L, Lou H. Enhancement of gastrointestinal absorption of quercitin by solid lipid nanoparticles. J Control Release. 2009;133(3):238–44.
7. Ying XY, Cui D, Yu L, Du YZ. Solid lipid nanoparticles modified with chitosan oligosaccharides for the controlled release of doxorubicin. Carbohydr Polym. 2011;84(4):1357–64.
8. Santander-Ortega MJ, Lozano-Lopez MV, Bastos-Gonzalez D, Peula-Garcia JM, Ortega-Vinuesa JL. Novel core-shell lipid chitosan and lipid-poloxamer nanocapsules: stability by hydration forces. Colloid Polym Sci. 2010;288(2):159–72.
9. Wu LF, Tang C, Yin CH. Folate-mediated solid–liquid lipid nanoparticles for paclitaxel-coated poly (ethylene glycol). Drug Dev Ind Pharm. 2010;36(4):439–48.
10. Zhang WL, Liu JP, Li SC, Chen MY, Liu H. Preparation and evaluation of stealth tashinone IIA-loaded solid lipid nanoparticles: influence of Poloxamer 188 coating on phagocytic uptake. J Microencapsul. 2008;25(3):203–9.
11. Nobuto H, Sugita T, Kubo T, Shimose S, Yasunaga Y, Murakami T, *et al*. Evaluation of systemic chemotherapy with magnetic liposomal doxorubicin and a dipole external electromagnet. Int J Cancer. 2004;109(4):627–35.
12. Zhang JQ, Zhang ZR, Yang H, Tan QY, Qin SR, Qiu XL. Lyophilized paclitaxel magnetoliposomes as a potential drug delivery system for breast carcinoma via parenteral administration: *in vitro* and *in vivo* studies. Pharm Res. 2005;22(4):573–83.
13. Cavalli R, Caputo O, Gasco MR. Solid lipospheres of doxorubicin and idarubicin. Int J Pharm. 1993;89(1):9–12.
14. Miglietta A, Cavallib R, Boccaa C, Bocca C, Gabriel L, Gasco MR. Cellular uptake and cytotoxicity of solid lipid nanospheres (SLN) incorporating doxorubicin or paclitaxel. Int J Pharm. 2000;210(1–2):61–7.
15. Uagio E, Cavalli R, Gasco MR. Incorporation of cyclosporin A in solid lipid nanoparticles (SLN). Int J Pharm. 2002;241(2):341–4.
16. Westesen K, Siekmann B. Investigation of the gel formation of phospholipid-stabilized solid lipid nanoparticles. Int J Pharm. 1997;151(1):35–45.
17. Zhao S, Yang CQ, Yan JW, Wang J. A novel solvethermal method for the preparation of magnetic monodisperse Fe_3O_4 nanoparticles II: High-surface-activity ferrihydrite used as precursor. Mater Res Bull. 2013;48(10):4385–9.
18. Manjunath K, Venkateswarlu V. Pharmacokinetics, tissue distribution and bioavailability of clozapine solid lipid nanoparticles after intravenous and intraduodenal administration. J Control Release. 2005;107(2):215–28.
19. Liu SL, Zhang LN, Zhou JP, Wu RX. Structure and properties of cellulose/Fe_2O_3nanocomposite fibers spun via an effective pathway. J Phys Chem C. 2008;112(12):4538–44.
20. Wang L, Yang CQ, Wang J. Effects of loading procedures of magnetic nanoparticles on the structure and physicochemical properties of cisplatin magnetic liposomes. J Microencapsul. 2012;29(8):781–9.
21. Jenning V, Mäder K, Gohla SH. Solid Lipid Nanoparticles (SLN) based on binary mixtures of liquid and solid lipids: a (1)H-NMR study. Int J Pharm. 2000;205(1–2):15–21.
22. García-Fuentes M, Torres D, Alonso MJ. Design of lipid nanoparticles for the oral delivery of hydrophilic macromolecules. Colloid Surf B. 2002;27(2–3):159–68.
23. Mehnert W, Mäder K. Solid lipid nanoparticles-production, characterization and applications. Adv Drug Deliv Rev. 2001;47(2–3):165–96.
24. Schwarz C, Mehnert W, Lucks JS, Miiller RH. Solid Lipid Nanoparticles (SLN) for controlled drug delivery. I. Production, characterization and sterilization. J Control Release. 1994;30:83–96.
25. Bloch K, Bangham AD, Scherphof GL, Kennedy EP, Waite M, Hostetler KY. Lipids and mombranes: past. Presint and future. Amsterdam: Elsever; 1986. p. 336.
26. Wang W, Li LM, Li ZL, Xi SG. The molecular mechanisms of interaction between rare earth irons and DPPC liposome. Spectrosc Spectr Anal. 1993;13(5):51–4.
27. Neumann MG, Schmitt CC, Iamazaki ET. A Fuorescence study of the interactions between sodium alginate and surfactants. Permissions Repr. 2003;338(10):1109–13.
28. Thakkar VT, Shah PA, Soni TG, Parmar MY, Gohel MC, Gandhi TR. Goodness-of-fit model-dependent approach for release kinetics of levofloxacin hemihydrates floating tablet. Dissolut Technol. 2009;16(1):35–9.
29. Yokoyama M, Okano T, Sakurai Y, Suwa S, Kataoka K. Introduction of cisplatin into polymeric micelle. J Control Rel. 1996;39:351–6.
30. Hwang TL, Lee WR, Hua SC, Fang JY. Cisplatin encapsulated in phosphatidylethanolamine liposomes enhances the *in vitro* cytotoxicity and *in vivo* intratumor drug accumulation against melanomas. J Dermatol Sci. 2007;46:11–20.
31. Vasir JK, Reddy MK, Labhasetwar VD. Nanosystems in drug targeting: opportunities and challenges. Curr Nanosci. 2005;1(1):47–64.